Supplementary Information

Preparations of Fluorine-doped α-Ni hydroxides as Alkaline Water Electrolysis Catalysts via Liquid Phase Deposition Method

Tomoyuki Watanabe[1], Kenko Tsuchimoto[2], Tomohiro Fukushima[2], Kei Murakoshi[2], Minoru Mizuhata[1], and Hiro Minamimoto[1]*

[1]Department of Chemical Science and Engineering, Graduate School of Engineering, Kobe University, 1-1 Rokkodai-cho, Nada, Kobe, 657-8501, Japan.

[2]Department of Chemistry, Faculty of Science, Hokaido University, North 10 West 8, kita-ku, Sapporo, Hokkaido, 060-0810, Japan,

1. Electrochemical properties of the prepared thin films.

Figure 1S shows Nyquist plots of thin film electrodes prepared by both pH conditions obtained in 1 M KOH solution. All plots were fitted to an equivalent circuit consisting of a solution resistance component and two capacitance/resistance parallel components (FTO substrate / nickel hydroxide thin film). On the film prepared with pH = 7.5, the large semicircle originating from the contact resistance of secondary particles adhered to the surface of the electrode was observed. For the case of the film prepared with lower pH condition, the charge transfer resistance was estimated to be around 7 Ω. From these investigations, the different conductivities, resulting in the different OER activity, depending on the reaction conditions were confirmed.

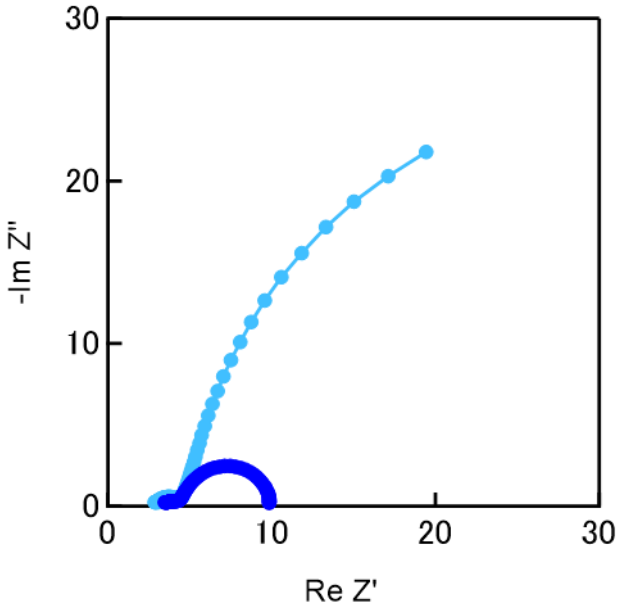

Fig. S1 | Nyquist plots of thin film prepared with each pH condition. The light and dark blue plots correspond to the films deposited in the parent solutions of pH = 7.5 and 6.8, respectively. The electrolyte solution was 1 M KOH and the electrochemical potential was set to 1.5 V.

2. Benchmarking OER electrode activities for various types of α-$Ni(OH)_2$

In Table S1, we present the Tafel slope values of α-$Ni(OH)_2$ obtained through different methods, including our own. Notably, our synthesized material exhibits the lowest Tafel slope among all reported values despite being prepared using gentle conditions, deposited on low-conductive substrates, and without any metal doping. Therefore, this comparison highlights the superiority of our current aqueous solution process.

Table S1 | Benchmarking of OER performance of α-$Ni(OH)_2$ materials prepared by various methods.

Materials	Doping Metal	Electrolyte	Preparation procedure, conditions	Tafel slope (mV / dec)	Ref.
α-$Ni(OH)_2$ on FTO	—	6 M KOH	LPD (r. t. ~ 50 °C)	52.1	This work
α-$Ni(OH)_2$ on Ni grid	—	6 M KOH	Thermal and high-pressure treatments (~10 MPa, ~ 130 °C)	54.0	29
2D α-$Ni(OH)_2$ nanosheet	—	1 M KOH	Lamellar reverse micelles method (r. t., ~ 170 °C)	77.4	30
1D α-$Ni(OH)_2$ nanobelt	Fe	1 M KOH	Hydrothermal reactions (at 120 °C)	67.4	S1
α-$Ni(OH)_2$ on $NiSe_2$	—	1 M KOH	Electrodeposition of $NiSe_2$ (-10 mA cm^{-2})	52.8	S2
α-$Ni(OH)_2$ on Ni foam	W	1 M KOH	Electrodeposition (r. t., -100 mA cm^{-2})	43.6	S3
$Ni(OH)_2$ hierarchical nanoarrays	Fe	1 M KOH	Chemical reduction	64.3	S4
$Ni(OH)_2$ nanosheet	Fe	1 M NaOH	Liquid phase exfoliation	60.0	S5
$Ni(OH)_2$ on Ni foam	—	6 M KOH	Hydrothermal reactions (at 150 °C)	62.0	S6

3. Characterizations of prepared films after OER tests

SEM images of thin films prepared with each pH condition as shown in Fig. 2S. In both cases, the acicular structures were still remained, indicating the relatively high stability of deposited films. Figure S3 showed the structural characterizations of films after OER tests. In XPS spectra (Fig. S3a), the remained Ni peaks were observed. Because we deposited Ni hydroxides on FTO substrates, at present, it is difficult to define the origin of F peaks. In addition, from XRD patterns, we found that the alpha phase partially changed to beta phase because the alpha Ni hydroxide easily transforms to beta phase. From these characteristics, it can be said that our prepared samples could be used as the model system to further investigations.

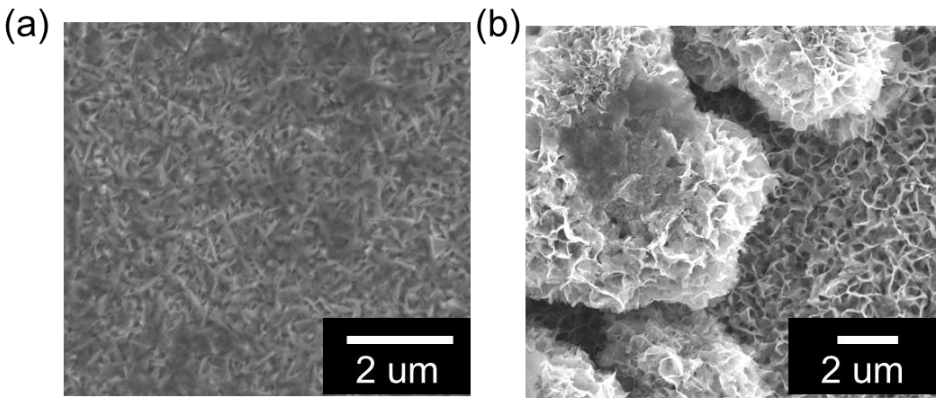

Fig. S2 | SEM images of thin films prepared with the parent solutions of pH = (a) 6.8 and (b) 7.5 after the electrochemical measurements shown in Fig. 3.

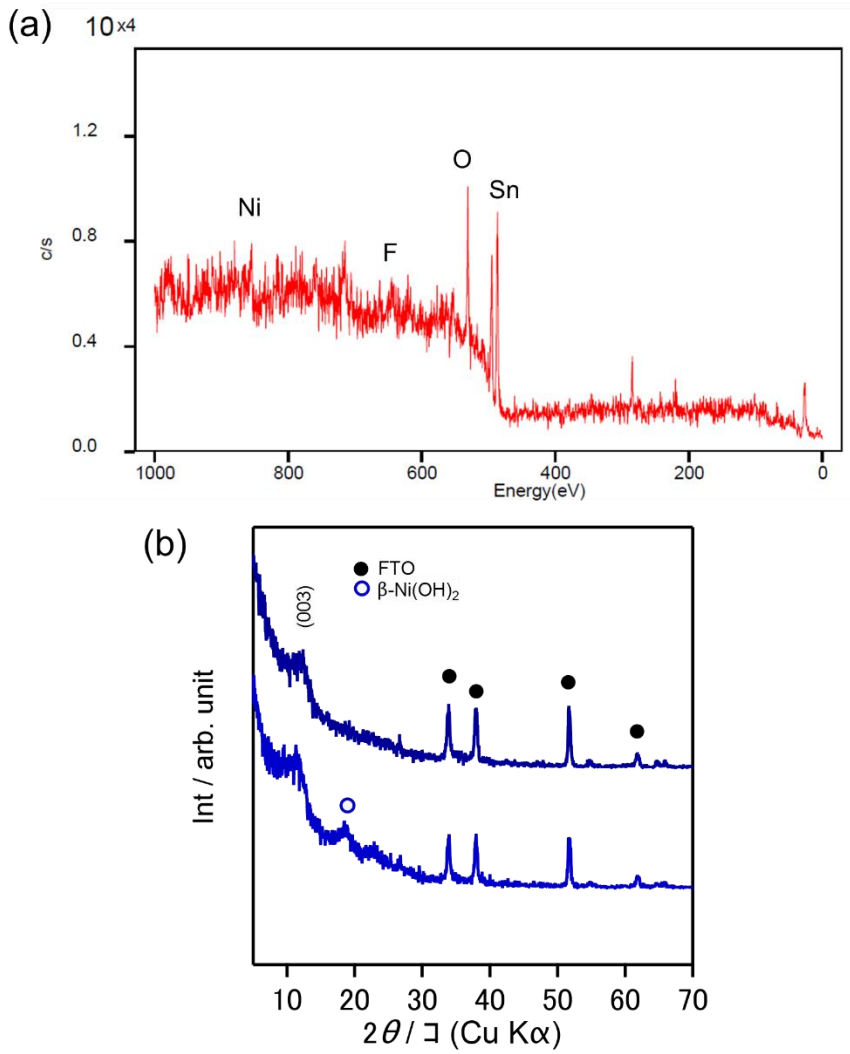

Fig. S3 | (a) XPS spectrum and (b) XRD patterns of the thin film prepared with pH = 6.8 obtained after OER tests. (b) The upper and bottom patterns correspond to the film before and after OER tests, respectively.

4. EDX mappings of the prepared film

The EDX mapping measurements were conducted using both samples as shown in Fig. 1S. As can

be found from figures, the uniform distributions of both Ni and F were confirmed in both pH condition cases. However, in the case for the film prepared with the parent solution of pH = 7.5, it was found that the large secondary particle mainly consisted with fluorine (Fig. 1Sb). Because the compositions of the reaction solutions were quite simple, this secondary particle would be the ammonium fluorine salt that was deposited within the reaction solution.

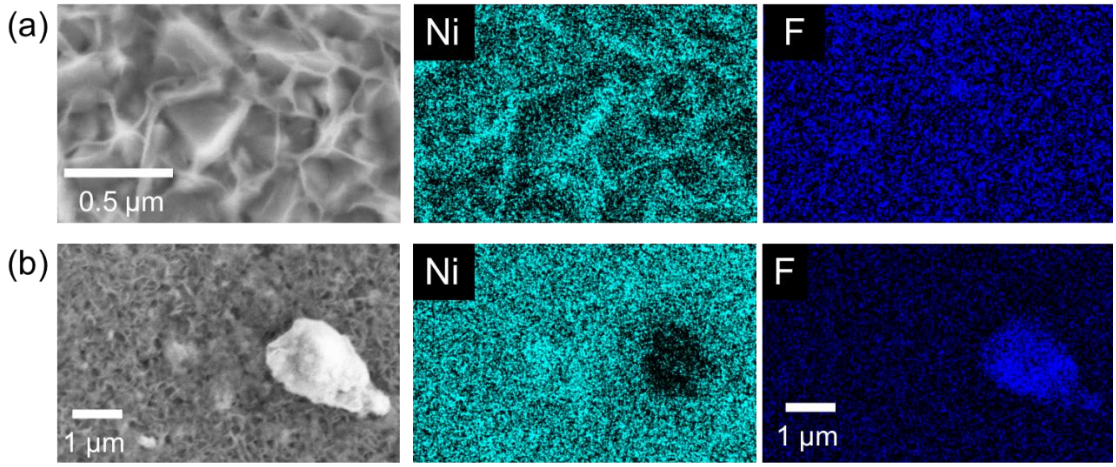

Fig. S4 | CV curves for α-$Ni(OH)_2$ films prepared with the parent solution of pH = 6.8. The electrochemical potential was scanned from 1.1 to 2.5 V for 10 times in KOH aqueous solutions.

Reference

S1. Wu, D.; Shen, X.; Liu, X.; Liu, T.; Luo, Q.; Liu, D.; Ding, T.; Chen, T.; Wang, L.; Cao, L.; Yao, T. Insight into Fe Activating One-Dimensional α-$Ni(OH)_2$ Nanobelts for Efficient Oxygen

Evolution Reaction. *J. Phys. Chem. C* **2021**, *125* (37), 20301–20308. https://doi.org/10.1021/acs.jpcc.1c05148.

S2. Wang, L.; Wang, X.; Xi, S.; Du, Y.; Xue, J. α-$Ni(OH)_2$ Originated from Electro-Oxidation of $NiSe_2$ Supported by Carbon Nanoarray on Carbon Cloth for Efficient Water Oxidation. *Small* **2019**, *15* (34), 1–8. https://doi.org/10.1002/smll.201902222.

S3. Wang, F.; Zhang, K.; Li, S.; Zha, Q.; Ni, Y. W-Doped α-$Ni(OH)_2$ Honeycomb-like Microstructures for Promoted Electrochemical Oxygen Evolution. *ACS Sustain. Chem. Eng.* **2022**, *10* (31), 10383–10392. https://doi.org/10.1021/acssuschemeng.2c03166.

S4. Zhou, T.; Cao, Z.; Zhang, P.; Ma, H.; Gao, Z.; Wang, H.; Lu, Y.; He, J.; Zhao, Y. Transition Metal Ions Regulated Oxygen Evolution Reaction Performance of Ni-Based Hydroxides Hierarchical Nanoarrays. *Sci. Rep.* **2017**, *7*, 1–9. https://doi.org/10.1038/srep46154.

S5. Harvey, A.; He, X.; Godwin, I. J.; Backes, C.; McAteer, D.; Berner, N. C.; McEvoy, N.; Ferguson, A.; Shmeliov, A.; Lyons, M. E. G.; Nicolosi, V.; Duesberg, G. S.; Donegan, J. F.; Coleman, J. N. Production of $Ni(OH)_2$ Nanosheets by Liquid Phase Exfoliation: From Optical Properties to Electrochemical Applications. *J. Mater. Chem. A* **2016**, *4* (28), 11046–11059. https://doi.org/10.1039/C6TA02811J.

S6. Al-Hejri, T. M.; Shaikh, Z. A.; Al-Naggar, A. H.; Raut, S. D.; Siddiqui, T.; Danamah, H. M.; Jadhav, V. V.; Al-Enizi, A. M.; Mane, R. S. Electrochemical Supercapacitor and Water Splitting Electrocatalysis Applications of Self-Grown Amorphous $Ni(OH)_2$ Nanosponge-Balls. *Electrochim.*

Acta **2024**, *474*, 143516. https://doi.org/10.1016/j.electacta.2023.143516.